processes

MDPI

Article

Comparative Analysis of Sulfuric Acid Alkylation Technologies Based on a Reaction Kinetic Model

Wenbin Zhang and Hongbo Jiang *

Research Institute of Petroleum Processing, School of Chemical Engineering, East China University of Science and Technology, Shanghai 200237, China; 15728067231@163.com
* Correspondence: hbjiang@ecust.edu.cn

Abstract: As a core component of transportation fuels, clean gasoline plays a vital role in environmental protection. Alkylate, with its nearly zero sulfur, aromatic, and olefin contents, coupled with its superior research octane number, serves as an ideal blending component for clean gasoline. This study established a kinetic model for sulfuric-acid-catalyzed isobutane–butene alkylation based on the carbocation reaction mechanism, incorporating 20 lumped components and 37 reaction pathways. Reactor models were developed to reflect the design characteristics of STRATCO and SINOALKY technologies. The model parameters were estimated using industrial operational data via the non-linear least-squares method. The validation results demonstrated excellent agreement with industrial values, showing average relative deviation rates of 1.72% (STRATCO) and 1.73% (SINOALKY) for C_8 product prediction. A prediction analysis revealed that selectivity and alkylate octane number of C_8 exhibit positive correlations with the isobutane-to-olefin ratio, acid-to-hydrocarbon ratio, and space–time relationship. It was also found that the internal circulation in the STRATCO technology enables thorough contact between the acid and hydrocarbon phases, while the multi-stage feeding in the SINOALKY technology maintains a favorable isobutane-to-olefin ratio. Both features are conducive to the alkylation reaction, enhancing the selectivity and octane number of C_8. These trends align with the intrinsic reaction principles of sulfuric-acid-catalyzed alkylation systems, providing theoretical guidance for alkylate production optimization.

Keywords: butene; isobutane; sulfuric acid; alkylation; kinetic model

check for updates

Academic Editor: Vincenzo Russo

Received: 28 April 2025
Revised: 16 May 2025
Accepted: 19 May 2025
Published: 21 May 2025

Citation: Zhang, W.; Jiang, H. Comparative Analysis of Sulfuric Acid Alkylation Technologies Based on a Reaction Kinetic Model. *Processes* **2025**, *13*, 1604. https://doi.org/10.3390/pr13051604

Copyright: © 2025 by the authors. Licensee MDPI, Basel, Switzerland. This article is an open access article distributed under the terms and conditions of the Creative Commons Attribution (CC BY) license (https://creativecommons.org/licenses/by/4.0/).

1. Introduction

In the context of the global energy transition driven by the imperative to reduce environmental harm, clean gasoline, as a core component of transportation fuels, is becoming increasingly important. Clean gasoline must meet stringent standards of having low sulfur, low aromatic, and low olefin contents and high octane numbers to reduce the emissions of tail gas pollutants and enhance its combustion efficiency [1]. Alkylate, with its nearly zero contents of sulfur, aromatics, and olefins, as well as its excellent research octane number (RON), has become an ideal blending component for clean gasoline [2]. Currently, the industrial alkylation technologies are mainly divided into solid–acid methods and liquid–acid methods [3]. Although solid–acid catalysts (such as molecular sieves and heteropolyacids) have environmental advantages, they are limited by problems such as the ease of carbon deposition, deactivation of active sites, and high regeneration costs, and have not yet achieved large-scale industrial application [4]. In the case of liquid–acid methods, the hydrofluoric acid method faces strict safety and environmental restrictions

due to its high toxicity, strong corrosiveness, and leakage risks [5]. While the ionic liquid method has low corrosiveness, it is difficult to promote due to the high synthesis costs and stringent requirements for raw materials [6]. In contrast, the sulfuric acid method, with its mature technical system, high raw material compatibility, and relatively controllable operational risks, is still the main choice for alkylation technologies in China [7,8], such as STRATCO (DuPont) technology and SINOALKY (Research Institute of Petroleum Processing, SINOPEC) technology [4]. Through the designs of circulation reactors and multi-stage reactors, respectively, the two technologies have their own characteristics in high-throughput processing and product regulation, providing reliable technical support for the production of clean gasoline.

Sulfuric-acid-catalyzed alkylation is a complex reaction system. It involves a series of reactions with carbocation intermediates, such as olefin polymerization, macromolecular cracking, and reactions with the sulfuric acid catalyst [9–11]. The mass transfer of isobutane to the acid phase is generally recognized as the rate-determining step [12]. Moreover, factors such as the micro-mixing of acid and hydrocarbon, reaction temperature, acid concentration, acid-to-hydrocarbon ratio, and alkane-to-olefin ratio also exert a substantial impact on the reaction yield [13–15]. The study of alkylation reaction kinetics serves as a crucial means to elucidate the alkylation mechanism, and numerous researchers have conducted in-depth investigations in this field. In the 1940s, Schmerling [16] pioneered the proposal of a chain reaction mechanism based on carbocations to explain the alkylation process, which was divided into three distinct stages: chain initiation, chain propagation, and chain termination. In the early 1970s, Langley et al. [17] utilized a carbocation model to describe the alkylation reaction between propylene and isobutane and determined the rate constants through the steady-state approximation method. In the late 1970s, Lee et al. [18], taking into account the addition reaction between olefins and alkanes, as well as the olefin polymerization reaction, experimentally calculated the model parameters. Sun et al. [19] explored the reaction kinetics of the sulfuric-acid-catalyzed alkylation in a batch-stirred reactor. They established a kinetic model based on the carbocation reaction mechanism to predict the variations in the contents of three key components, namely trimethylpentanes, dimethylhexanes, and heavy ends. Xin et al. [20] established a kinetic model for the sulfuric-acid-catalyzed alkylation reaction, performing a more detailed lumping of high-carbon components (C_9–C_{11}) and low-carbon components (C_5–C_7). In 2024, Ma et al. [9] estimated the detailed kinetic constants for H_2SO_4-catalyzed alkylation systems with and without the surfactant $[N_{1,1,1,1}][C_{10}SO_4]$. They developed a kinetic model based on the carbocation reaction mechanism to predict variations in three key component concentrations. However, their model exhibited an oversimplified lumped component classification process and incomplete consideration of low-carbon components (C_5–C_7).

This paper is based on the carbocation reaction mechanism, which is used to construct a detailed kinetic model for the sulfuric-acid-catalyzed alkylation of isobutane and butene. In the model-solving process, the sequential modular (SM) method reduces the dependency on initial guesses due to its stepwise solution approach, demonstrating operational simplicity in straightforward processes. However, when handling systems with recycling streams (e.g., acid–hydrocarbon recycling in alkylation processes), the SM method suffers from decreased convergence efficiency and prolonged computational times due to iterative recirculation. In contrast, the equation-oriented (EO) method improves the computational efficiency by globally solving non-linear equations simultaneously. Given these considerations, this study adopts the EO method for model development. Through a parameter analysis, the crucial role of reactor design (such as the circulation flow rate of the STRATCO technology and multi-stage feeding of the SINOALKY technology) in

the primary alkylation reaction is revealed, and the effect of the operating parameters on product distribution is investigated.

2. Industrial Alkylation Technology

2.1. STRATCO Alkylation Technology

The STRATCO alkylation technology was developed by DuPont Co. in the United States [21,22], and the industrial equipment was sourced from Daekyung Machinery & Engineering Co., Ltd. (Ulsan 2nd Plant, Ulsan 45009, Republic of Korea). Operational data, including for the feed and product composition, temperature, pressure, and acid concentration, were collected from an industrial facility with an annual processing capacity of 300,000 tons. The unit comprises three parallel reactors, each structured as shown in Figure 1 [23], where the hydrocarbon feedstock flows in parallel into all reactors. In contrast, the sulfuric acid follows in a different feeding strategy, whereby the sulfuric acid is injected into the first and second reactors in parallel; after leaving the two reactors, it enters the third reactor. Although this configuration reduces the acid concentration in the third reactor by 1–2 wt% compared to the preceding reactors, it achieves an optimal balance between the catalyst utilization efficiency and side reaction suppression. Finally, the product streams from the three reactors are combined into a single stream.

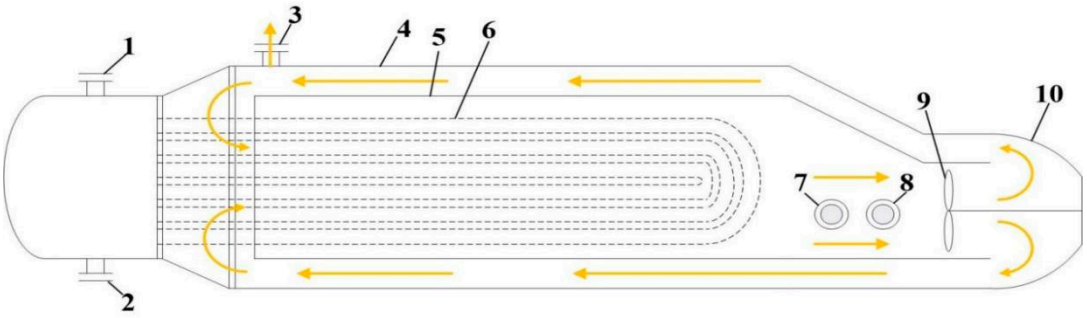


Figure 1. STRATCO alkylation reactor. 1—tube side outlet; 2—tube side inlet; 3—reactor outlet; 4—shell; 5—draft tube; 6—U-tube bundles; 7—Sulfuric acid inlet; 8—hydrocarbon inlet; 9—impeller; 10—hydraulic head.

The STRATCO alkylation technology achieves efficient reaction control and product refinement through three key engineering designs. First, enhanced thermal management is realized via U-tube heat exchangers, where shell-side fluid interactions rapidly dissipate the reaction heat, ensuring a uniform temperature distribution and suppressing side reactions caused by localized overheating. Second, synergistic mixing–circulation integration employs a high-shear impeller to emulsify the acid–hydrocarbon biphasic system through turbulence, while high-velocity circulation homogenizes the temperature field. Third, an integrated post-treatment system combines multistage sedimentation for acid recovery with caustic washing and water washing to remove acidic residues, ultimately yielding high-purity alkylate oil. Through the systematic coordination of heat transfer, mass transfer, and separation, this technology demonstrates robust operational stability and flexibility in industrial-scale applications.

Sixty-two sets of industrial data from the STRATCO alkylation unit (April 2020–February 2021) were collected for modelling, as follows: feed flow rates of 30–70 t/h per reactor; inlet and outlet temperatures maintained at 2.0–4.0 °C and 6.0–6.5 °C, respectively; isobutane-to-olefin molar ratio regulated between 7.1:1 and 12.1:1; acid-to-hydrocarbon volumetric ratio remained stable at 1.1:1, with acid concentrations (wt%) of 92–96% in the acid phase of the preceding two reactors and 1–2 percentage reductions in acid concentration in the third reactor; system pressure stabilized at 0.48 MPa, ensuring a liquid-phase state

without significantly altering the reaction pattern. Structurally, the reactor system allocates half of its space to the internal volume spanning from the hydrocarbon phase inlet to the reactor outlet, a design that enhances the circulating flow and micro-interface mass transfer to facilitate efficient carbocation reactions under low-temperature conditions.

2.2. SINOALKY Alkylation Technology

The SINOALKY alkylation technology [24], developed by Sinopec Co., employs a three-stage reactor with an "N"-shaped static mixing configuration (Figure 2), although the third-stage inlet valve remains closed in the actual unit, with an annual processing capacity of 200,000 tons. At the first-stage inlet of the reactor, a static mixer (highlighted in Figure 2) homogenizes blended feeds—comprising fresh feedstock, recycled hydrocarbons, and sulfuric acid—to initiate acid–hydrocarbon emulsion formation and primary reactions. The first-stage effluent is subsequently mixed with supplementary fresh feedstock and directed to the second stage.

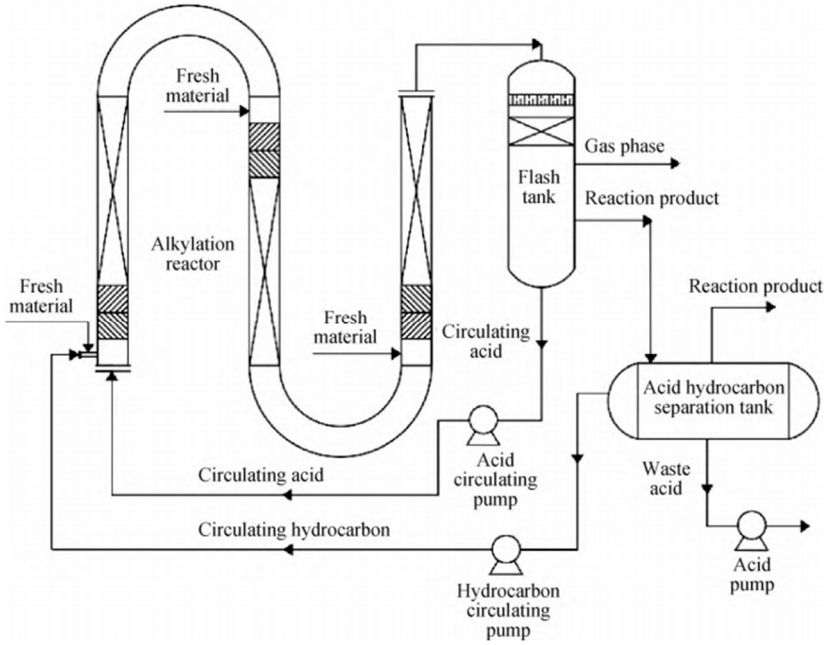


Figure 2. Alkylation reactor of SINOALKY technology.

The SINOALKY alkylation technology achieves efficient reaction control and product refinement through three key engineering designs. First, the vertical flow channel design minimizes acid–hydrocarbon phase separation by redirecting the process fluid, thereby enhancing the interfacial stability. Second, the N-shaped folded flow channel configuration reduces the reactor's vertical height, significantly lowering the pump head requirement. Third, the supplementary feed injection at the second stage locally dilutes the olefin concentration, elevating the isobutane-to-olefin ratio to suppress oligomerization side reactions.

Twenty-nine sets of industrial data from the SINOALKY alkylation unit (January–October 2022) were collected for modelling: The total material flow rates ranged from 630–780 t/h, comprising the fresh feed (110–130 t/h) and recycled hydrocarbons (500–650 t/h). The fresh feed exhibited an isobutane-to-butene molar ratio of 10.0:1–14.5:1, supplemented by trace C_5 components and inert substances. The reactor inlet and outlet temperatures were maintained at 1.0–4.5 °C and 2.5–6.0 °C, respectively, with the operating pressure stabilized at 0.32–0.42 MPa, an acid-to-hydrocarbon volumetric ratio of 1.1:1,

and a sulfuric acid concentration (wt%) range of 91–93%. The reactor has an N-shaped three-stage design (stage 1: 32.988 m^3; stage 2: 32.017 m^3; stage 3: 19.339 m^3).

3. Modelling Methodology

3.1. Reactor Model

3.1.1. STRATCO Reactor Model

To address the challenge of directly observing the internal circulating flow in STRATCO reactors, Cai and Dai [25] conducted computational fluid dynamics (CFD) simulations using the standard k–ε turbulence model. Their study established a quantitative relationship between the draft tube circulating flow rate and impeller operating parameters. The numerical results demonstrated a positive correlation between the circulating flow rate and impeller rotational speed. Based on the fluid flow state and structural characteristics inside the reactor, the reactor can be simplified to a plug flow reactor with circulation, and its structure is shown in Figure 3. Based on the actual flow characteristics of the STRATCO alkylation reactor, this paper puts forward the following assumptions:

(a) Hydrocarbon-phase and acid-phase flows are modelled using a plug flow reactor (PFR) approach, with undetectable olefin concentrations at the outlet—indicating that the alkylation reactions are completed.

(b) Given the typical industrial practice of maintaining constant impeller speeds, the circulating flow rate in the draft tube can be assumed as a fixed value.

(c) The STRATCO reactor maintains near-isothermal conditions by extracting heat generated from alkylation reactions in the shell side through the reaction effluent in U-tubes, while the impeller-driven high fluid velocity ensures efficient heat removal, thereby stabilizing the shell-side temperatures. Distributed control system (DCS) data reveal that the temperature does not change significantly across the reactor, justifying the isothermal reactor assumption.

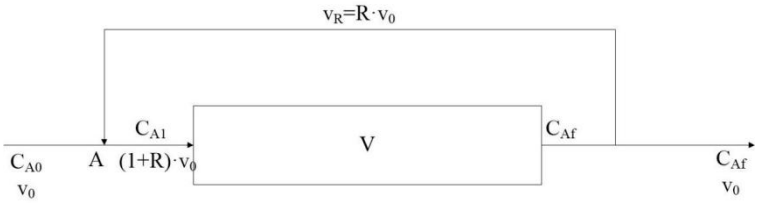


Figure 3. Model of the STRATCO alkylation reactor.

3.1.2. SINOALKY Reactor Model

The SINOALKY alkylation reactor model (Figure 4) features an adiabatic tubular structure operating under turbulent flow conditions (Re > 28,000). The sulfuric acid (continuous phase) and hydrocarbons (dispersed phase) rapidly form stable emulsions. The sufficiently large acid–hydrocarbon interfacial contact area justifies neglecting the radial (perpendicular to flow direction) concentration gradient and corresponding temperature gradient. The reactor's segmented design exhibits length-to-diameter (L/D) ratios of 10.5 (stages 1–2) and 7.2 (stage 3), yielding a cumulative L/D ratio of 28.2. This configuration generates axially uniform velocity profiles due to the dominance of turbulent flow. With negligible axial back-mixing [26], the system can be approximated as a plug flow reactor (PFR). Static mixers at each stage allow the sulfuric acid and hydrocarbon to be fully mixed, significantly enhancing the contact efficiency. Notably, rapid primary reactions dominate the front section of each stage, while slower side reactions in mid-to-rear sections render the mass transfer effects negligible under these conditions. For heat transfer, thermal dispersion was not considered in this paper for the following reasons: (1) the dilution effects due to

the flow rate of the recycled streams (hydrocarbons and sulfuric acid) being much over that of the fresh feed, which suppresses rapid temperature increases; (2) the negligible radial temperature gradients owing to reactor insulation.

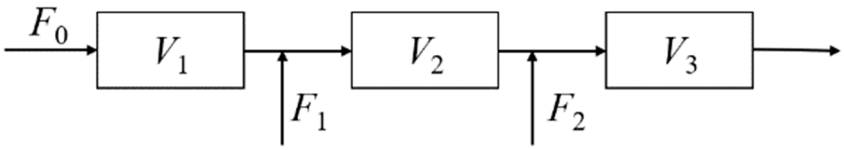


Figure 4. Model of the SINOALKY alkylation reactor.

Based on the actual flow characteristics of the SINOALKY alkylation reactor, the following assumptions are proposed in this paper:

(a) The reactor is a plug flow reactor with three-stage feeding. The radial concentration distribution inside is uniform, and only the changes in concentration and temperature along the axial flow direction are considered.

(b) In a typical alkylation process, the reactor internals are characterized by a sulfuric acid continuous phase and a hydrocarbon dispersed phase. Therefore, the acid-to-hydrocarbon ratio is operationally controlled within the range of 1.1–1.2. At the inlet of the SINOALKY reactor, the acid and hydrocarbon phases are rapidly homogenized into an emulsion phase via a static mixer, creating a pseudo-homogeneous fluid. The liquid-phase reaction system of sulfuric-acid-based alkylation is treated as a pseudo-homogeneous phase. The sulfuric acid concentration has a significant impact on the catalytic reaction rate.

To calculate the axial temperature variation in a plug flow adiabatic reactor, it is necessary to estimate the reaction heats of various reactions in the alkylation reaction system. The enthalpy values of each hydrocarbon molecule and ion required for calculating the reaction heat are estimated using Gaussian 09W (Gaussian Inc., Wallingford, CT, USA) and GaussView 5.0 [27]. The differential expression of the reaction temperature with respect to the residence time is shown in Equation (1). The calculated enthalpy changes for each reaction at 3.5 °C are listed in Table 1. The 37 equation numbers in the Table 1 correspond to 37 reaction equations.

$$\frac{dT}{d\tau} = \sum_{i=1}^{37}(r_i)(-\Delta H_{r,i}) \times \frac{M_c}{M_s} \div C_p \quad (1)$$

where T is the temperature, in K; τ is the residence time of the liquid-phase reaction, in min; r_i is the reaction rate of the i-th reaction, in mol/(kg·min); $\Delta H_{r,i}$ is the reaction heat of the i-th reaction equation, in J/mol; M_c is the total mass of hydrocarbon materials in the specific stage of reactor, in kg; M_s is the total mass of hydrocarbon materials and sulfuric acid materials in the specific stage of the reactor, in kg; C_p is the average specific heat capacity, in J/(kg·K).

Table 1. Reaction heat (3.5 °C).

Equation Number	ΔH_r/KJ·mol^{-1}	Equation Number	ΔH_r/KJ·mol^{-1}	Equation Number	ΔH_r/KJ·mol^{-1}
1	−97.44	14	−10.14	27	−69.45
2	97.44	15	−16.31	28	−67.24
3	−92.58	16	1.82	29	−61.07
4	−86.41	17	7.99	30	−89.52

Table 1. *Cont.*

Equation Number	ΔH_r/KJ·mol^{-1}	Equation Number	ΔH_r/KJ·mol^{-1}	Equation Number	ΔH_r/KJ·mol^{-1}
5	6.44	18	−11.63	31	−92.14
6	−89.58	19	−5.47	32	−93.54
7	8.78	20	1.87	33	0.06
8	−51.67	21	8.04	34	2.86
9	−57.83	22	−11.58	35	5.47
10	−65.13	23	−5.42	36	0.75
11	−71.29	24	−94.67	37	−95.00
12	3.31	25	−88.51		
13	−2.85	26	−75.61		

The average specific heat capacity of the reactor fluid stream was determined based on the inlet composition of each reactor section (including sulfuric acid and hydrocarbons), along with the heat capacities of individual components. Due to the presence of numerous isomers in the hydrocarbon stream at the reactor inlet and the lack of detailed isomer-specific composition data for C_5^+ components in the collected datasets, representative components were selected to calculate the heat capacities of C_5^+ hydrocarbons. The specific components are listed in Table 2. The heat capacity calculation formula for C–H compounds within the alkylation reaction temperature range [28] is provided in Equation (2), while the formula for sulfuric acid [29] is given in Equation (3). Notably, the heat capacity of C-H compounds is expressed in J·mol^{-1}·K^{-1}, whereas the average specific heat capacity in Equation (1) uses J·kg^{-1}·K^{-1}.

$$C_{\mathrm{pL}} = A + BT + CT^2 + DT^3 \tag{2}$$

where C_{pL} is the heat capacity of liquid hydrocarbons, in J·mol^{-1}·K^{-1}; T is the temperature, in K; A, B, C, and D are equation coefficients, with specific values listed in Table 2 [28].

$$C_{\mathrm{ps}} = (A + Bt) \times 4185.85 \tag{3}$$

where C_{ps} is the heat capacity of sulfuric acid, in J·kg^{-1}·K^{-1}; t is the temperature, in °C; A and B are the equation coefficients, with specific values provided in Table 3 [29].

Table 2. Correlation coefficients between the hydrocarbon heat capacity and temperature for C–H compounds.

Component	A	$B \times 10^2$	$C \times 10^4$	$D \times 10^6$
Propane	59.6420	32.8310	−15.3770	3.6539
n-Butane	62.8730	58.9130	−23.5880	4.2257
Isobutane	71.7910	48.4720	−20.5190	4.0634
Isobutene	57.6110	56.2510	−22.9850	4.1773
1-Butene	74.5970	33.4340	−13.9140	3.0241
trans-2-Butene	36.1620	79.7390	−30.6740	4.8919
Isopentane	109.5040	11.7106	−0.8803	1.0706
Isoprene	90.0050	39.7770	−15.4620	2.9909
2,3-Dimethylbutane	115.6688	21.7756	−3.2285	1.3881
2,4-Dimethylpentane	155.9063	−17.8757	19.5046	−1.9530
2,2,4-Trimethylpentane	145.4385	13.3233	6.0554	0.0000
2,3-Dimethylhexane	109.6920	109.1100	−32.5790	4.1505

Table 2. *Cont.*

Component	A	$B \times 10^2$	$C \times 10^4$	$D \times 10^6$
2,2,5-Trimethylhexane	139.6900	86.3420	−26.0670	3.6252
Decane	325.6033	−29.6775	0.5202	2.7394
2-Methyldecane	464.6960	−196.4158	71.1196	−6.4211
Dodecane	84.4850	203.5800	−50.9810	5.2186

Table 3. Correlation coefficient between the sulfuric acid heat capacity and temperature.

Sulfuric Acid Concentration/wt.%	A	$B \times 10^4$	Sulfuric Acid Concentration/wt.%	A	$B \times 10^4$
80	0.437	4.4	90	0.386	4.3
82	0.440	3.5	92	0.366	4.7
84	0.437	2.4	94	0.347	4.9
86	0.419	3.4	96	0.334	5.0
88	0.403	3.9	98	0.325	5.0

3.2. Kinetic Model

Currently, the carbocation chain reaction theory [30,31] based on modern analytical techniques has become the main theoretical framework for the alkylation mechanism, which can also be applied for C_4 alkylation reaction systems.

In the chain initiation stage, the protons provided by sulfuric acid undergo an electrophilic addition reaction with butene to generate C_4 carbocation. Among them, the tert-butyl carbocation is the most stable.

In the chain growth stage, the tert-butyl carbocation, which is triggered by the addition reaction of the proton and butene, undergoes an addition reaction with isobutene to obtain a C_8 carbocation.

In the chain termination process, the generated C_8 carbocation continues to abstract the active hydride ion on isobutane to become a C_8 molecule. The isobutane that has lost the hydride ion becomes a tert-butyl carbocation and enters the next cycle.

In addition, along with the formation of the main alkylation product, competitive reaction paths such as the isomerization, β-cleavage, and oligomerization of carbocations not only lead to the generation of light components (C_5–C_7) and heavy components (C_9^+) but also significantly increase the isomer diversity of C_8 products through branch chain isomerization and skeletal rearrangement.

Therefore, using a detailed kinetic model for the C_4 alkylation reaction system will result in an excessive number of model parameters, thereby increasing the difficulty of the parameter estimation process. The lumping method is a method of grouping numerous chemical substances in a complex chemical reaction system into a few lumped pseudo-components according to the similarities between their reaction behaviors, and when investigating the reaction kinetics between the lumps [32].

After balancing the representation detail and computation efficiency of the kinetic model, the lumping method is selected to develop the kinetic model based on the analysis of industrial data for C_4 alkylation units. The following assumptions are proposed for the kinetic model:

(a) According to the daily analysis of the industrial data, the components in the reaction system are lumped based on the principle of similar kinetic characteristics in this study. Specifically, components with C_5 and above are classified according to the number of carbon atoms. Among them, as the main product, C_8 is mainly composed of trimethylpentane (TMP) and dimethylhexane (DMH), so it is divided into two lumped components, namely TMP and DMH. Components with less than 5 car-

bon atoms are lumped and classified according to specific components, with butene as an independent lumped component. Given that the alkylation reaction follows the carbocation reaction mechanism, a series of carbocations and olefin intermediates are generated during the reaction process, and these intermediates are also lumped separately. A total of 20 lumped components are finally classified, which are butene, TMP^+, DMH^+, isobutane, C_5, C_6, C_7, TMP, DMH, C_9, C_{10}, C_{11}, C_{12}, iC_4^+, iC_5^+, iC_6^+, iC_7^+, $iC_5^=$, $iC_6^=$, and $iC_7^=$.

(b) The isomerization reaction rates among the four isomers of butene are fast enough, so the four butene are considered to be in chemical equilibrium. The isomers of butene are grouped as one lumped component, and the contents of 1-butene, cis-2-butene, trans-2-butene, and isobutene can be calculated using the equilibrium constants.

(c) The cracking reactions of C_{12}^+ and C_{16}^+ follow the β-cracking rule. In the initial stage of the alkylation reaction, the tert-butyl carbocation (formed via olefin protonation) reacts with olefins to generate C_8 carbocations (C_8^+). These C_8^+ species further react with olefins to form larger carbocations (e.g., C_{12}^+, C_{16}^+). However, such high-carbon carbocations are unstable and undergo β-scission, yielding smaller olefins and intermediate carbocations. These intermediates subsequently participate in hydride transfer reactions with isobutane, ultimately forming alkanes such as C_5, C_6, and C_7 hydrocarbons.

(d) The reaction of TMP^+ (DMH^+) to generate C_{12}^+ is an instantaneous reaction.

(e) As inert components, the propane and n-butane in the raw materials do not participate in the alkylation reactions.

(f) The concentration effects of the hydrocarbon monomers and carbocation intermediates participating in the reactions are all first-order.

The alkylation reaction network constructed in this study is shown in Figure 5.

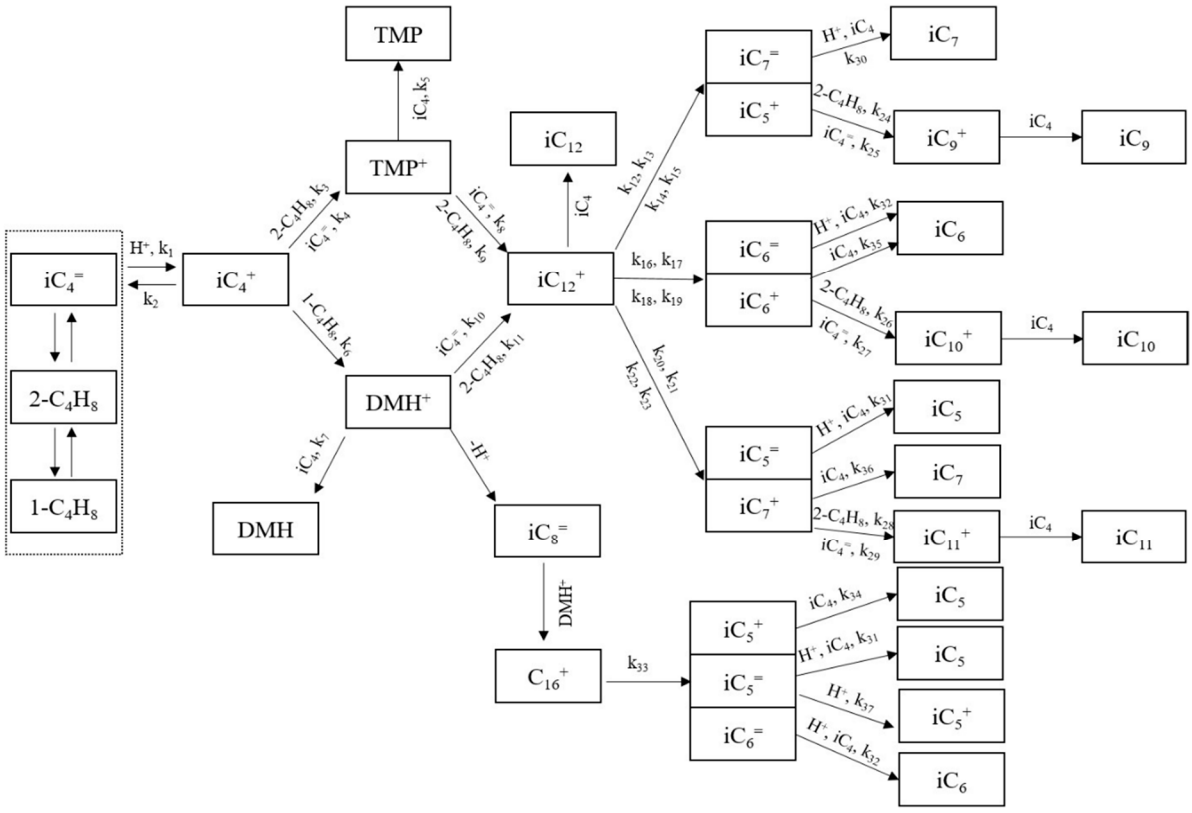


Figure 5. Alkylation reaction network.

In industrial operations, the sulfuric acid concentration and acid-to-hydrocarbon ratio exhibit minimal variation under stable unit performance, resulting in negligible impacts on reaction products. The correction function established by Xin [20] is introduced to reflect the influence of the acid concentration and acid-to-hydrocarbon ratio on the selectivity of the main reaction, as shown in Equation (4).

$$f(AO, wcor) = AO \cdot e^{wcor} \tag{4}$$

where AO represents the volume ratio of acid to hydrocarbons; $wcor$ is the re-normalized value of the acid concentration, and its range is 0.21–1.

According to the above reaction network, reaction rate equations corresponding to each reaction are shown in Equation (5).

$$r_i = k_i \cdot \prod c_g \tag{5}$$

where r_i represents the reaction rate of the i-th reaction (with a total of 37 reactions), in which r_3~r_7 are the main reactions; k_i denotes the rate constant of the i-th reaction; c_g indicates the set of lumped reaction species participating in the i-th reaction. The subscript g corresponds to the following lumped species: 1, butene; 2, TMP^+; 3, DMH^+; 4, isobutane; 5, iC_5; 6, iC_6; 7, iC_7; 8, TMP; 9, iC_9; 10, iC_{10}; 11, iC_{11}; 12, iC_{12}; 13, DMH; 14, iC_4^+; 15, iC_5^+; 16, iC_6^+; 17, iC_7^+; 18, $iC_5^=$; 19, $iC_6^=$; 20, $iC_7^=$.

Considering the effects of the sulfuric acid concentration and acid/hydrocarbon ratio on the overall reaction rate, combined with the reactor model established here, the obtained kinetic differential equation is shown in Equation (6).

$$\frac{d_{C_g}}{d_\tau} = \left(\sum r_j - \sum r_l\right) \cdot AO \cdot \omega \tag{6}$$

where τ is the residence time of the liquid-phase reaction, in min; c_g is the molality of species g, in mol/kg; ω is the concentration of sulfuric acid; r_j is the rate of reaction j producing species g, in mol/(kg·min); r_l is the rate of reaction l consuming species g, in mol/(kg·min). For the five main reaction rates (r_3, r_4, r_5, r_6, r_7), they must be multiplied by the correction function.

3.3. Model Transformation

The sequential modular method (SM) exhibits inherent limitations in convergence efficiency and computational time when applied to the iterative solution of cyclic systems, such as acid–hydrocarbon recycling processes. In contrast, the equation-oriented method (EO) solves the entire system of equations simultaneously, achieving global convergence with high computational efficiency. In view of this, this study adopted the EO method to develop the model. Based on the orthogonal collocation method [33,34], the differential equations for heat transfer and mass transfer were transformed into algebraic equations via spatial discretization.

The first derivative at any collocation point can be calculated by using the function values of all collocation points including this point, as shown in Equation (7) below.

$$\frac{d\boldsymbol{y}}{dx} = \boldsymbol{z}\boldsymbol{y} \tag{7}$$

where $\boldsymbol{z}$ is the coefficient matrix of the collocation points.

Given that the alkylation main reaction predominantly occurs in the front section of the reactor, the volumetric space within a STRATCO reactor or specific stage of a SINOALKY reactor is partitioned into two parts—the front 10% and rear 90%.

In each part, there are four internal collocation points and two boundary positions for one STRATCO reactor or a specific stage of SINOALKY reactor: $n(1) = 0$; $n(2) = 0.06943$; $n(3) = 0.33000$; $n(4) = 0.66999$; $n(5) = 0.93057$; $n(6) = 1$. The inlet composition $n(1) = 0$ of the second part corresponds to the outlet composition of the preceding part, where z is the corresponding coefficient matrix of the collocation points [35].

The space–time τx corresponding to the x-th point is:

$$\tau_x = \tau_{in} + (\tau_{out} - \tau_{in}) \cdot n(x) \tag{8}$$

The discretization results at the collocation point x are shown in Equations (9) and (10) below.

$$\frac{dTx}{d\tau} = \frac{dn(x)}{d\tau} \cdot \frac{dTx}{dn(x)} = \frac{1}{\tau_{\text{out}} - \tau_{\text{in}}} \cdot \sum_{y=1}^{N+2} z_{xy} T_y \tag{9}$$

$$\frac{dCx(j)}{d\tau} = \frac{dn(x)}{d\tau} \cdot \frac{dCx(j)}{dn(x)} = \frac{1}{\tau_{\text{out}} - \tau_{\text{in}}} \cdot \sum_{y=1}^{N+2} z_{xy} C_y(j) \tag{10}$$

For each part, a series of constraint equations can be constructed at each collocation point based on the mass conservation and energy conservation. For all internal collocation points (x = 2~6) within the same part, equality constraint equations are established based on the condition that the internal residuals are equal to zero, as shown in Equations (11) and (12).

$$R_{T,x} = \sum_{y=1}^{N+2} z_{xy} T_y - \frac{1}{\tau_{\text{out}} - \tau_{\text{in}}} \sum_{i=1}^{37} (r_x(i))(-\Delta H_{r,i}) \times \frac{M_C}{M_S} \div C_p = 0 \tag{11}$$

$$R_{C,x} = \sum_{y=1}^{N+2} z_{xy} C_y(j) - \frac{1}{\tau_{\text{out}} - \tau_{\text{in}}} \left(\sum r_j - \sum r_l\right) . AO . \omega = 0 \tag{12}$$

4. Results and Discussion

4.1. Parameter Estimation

There are a total of 37 reactions in the alkylation reaction network. Since the sulfuric acid, as the catalyst for the alkylation process, shows no difference except its concentration, the established kinetic model adopted the activation energies reported in the literature [36]. The activation energy of a reaction refers to the energy required for molecules to transition from their ground state to an activated state capable of undergoing chemical transformation. For elementary reactions, the activation energy corresponds directly to that of the elementary step. In contrast, for complex non-elementary reactions, the activation energy represents the apparent activation energy of the overall reaction, which is defined as the algebraic sum of activation energies from individual elementary steps. It is thought that the activation energy of some reactions involving the chain termination step is very small, so it can be reasonably assumed that their rate constants remain relatively stable within the range of reaction temperatures. However, the rate constants of the chain initiation and its reverse reactions (k_1, k_2), as well as the rate constants of the chain growth (k_3, k_4, k_6), need to be correlated with temperature changes through the Arrhenius formula. The rate constant, denoted as k, serves as a quantitative representation of the chemical reaction rate. Its physical significance lies in the equivalence of its numerical value to the reaction rate when all participating species are at unit concentration. Referring to the values in the literature [37], the activation energies used to calculate k_1, k_2, k_3, k_4, and k_6 are −45.14, 41.44, 103.44, 103.44, and 95.01 kJ/mol, respectively. Finally, initial values of the kinetic parameters are given, and the non-linear least-squares optimization algorithm is used for kinetic parameter estimation. The optimized objective function is the sum of squares of the

deviations between the model calculation results and the actual measured data from the commercial units, as shown in Equation (13).

$$F = \sum_i^n \sum_j^m (x_{i,j,exp} - x_{i,j,cal})^2 \quad (13)$$

where i = 1~n, indicating that there are n lumps; j = 1~m, indicating that there are m groups of data; $x_{i,j,exp}$ and $x_{i,j,cal}$ respectively denote the experimental value and the calculated value of the j-th group of data for the i-th lump.

The 62 industrial datasets from STRATCO (April 2020–February 2021) and 29 datasets from SINOALKY (January–October 2022) comprehensively cover the majority of the historical operating conditions. This operational diversity ensures the reliability of the kinetic model. Fifty-two sets of data out of the 62 industrial sets from the STRATCO alkylation unit and 24 sets of data out of the 29 industrial sets from the SINOALKY alkylation unit were selected to estimate the kinetic parameters of the model. The inlet temperatures of the STRATCO reactor range from 2.0 to 4.0 °C, while those of the SINOALKY reactor range from 1.0 to 4.5 °C. Supposing the reaction temperature is 3.5 °C, the estimated rate constant results are presented in Table 4. Figure 6 is a bar chart comparing key rate constants.

Table 4. Rate constants estimated for the STRATCO and SINOALKY reactors (3.5 °C).

Rate Constants	STRATCO	SINOALKY	Rate Constants	STRATCO	SINOALKY
k_1/min^{-1}	18.98	13.84	k_{20}/kg·mol^{-1}·min^{-1}	192.47	97.63
k_2/min^{-1}	10.99	12.65	k_{21}/kg·mol^{-1}·min^{-1}	132.26	95.05
k_3/kg·mol^{-1}·min^{-1}	336.53	469.22	k_{22}/kg·mol^{-1}·min^{-1}	84.24	98.01
k_4/kg·mol^{-1}·min^{-1}	578.66	493.56	k_{23}/kg·mol^{-1}·min^{-1}	96.30	98.02
k_5/kg·mol^{-1}·min^{-1}	1.60	1.54	k_{24}/kg^2·mol^{-2}·min^{-1}	26.04	139.32
k_6/kg·mol^{-1}·min^{-1}	10,028.01	22178.64	k_{25}/kg^2·mol^{-2}·min^{-1}	73.73	132.16
k_7/kg^2·mol^{-2}·min^{-1}	0.21	5.00	k_{26}/kg^2·mol^{-2}·min^{-1}	31.93	35.47
k_8/kg^2·mol^{-2}·min^{-1}	2.07	0.52	k_{27}/kg^2·mol^{-2}·min^{-1}	27.32	37.94
k_9/kg^2·mol^{-2}·min^{-1}	1.37	0.45	k_{28}/kg^2·mol^{-2}·min^{-1}	27.03	145.67
k_{10}/kg^2·mol^{-2}·min^{-1}	1.37	1.86	k_{29}/kg^2·mol^{-2}·min^{-1}	81.08	149.72
k_{11}/kg^2·mol^{-2}·min^{-1}	1.37	1.99	k_{30}/kg^2·mol^{-2}·min^{-1}	11.48	11.49
k_{12}/kg·mol^{-1}·min^{-1}	71.30	84.39	k_{31}/kg^2·mol^{-2}·min^{-1}	4.09	6.71
k_{13}/kg·mol^{-1}·min^{-1}	71.35	111.95	k_{32}/kg^2·mol^{-2}·min^{-1}	51.35	51.72
k_{14}/kg·mol^{-1}·min^{-1}	115.91	119.98	k_{33}/kg·mol^{-1}·min^{-1}	3486.21	3129.43
k_{15}/kg·mol^{-1}·min^{-1}	107.04	119.01	k_{34}/kg·mol^{-1}·min^{-1}	1.30	1.19
k_{16}/kg·mol^{-1}·min^{-1}	135.72	91.45	k_{35}/kg·mol^{-1}·min^{-1}	2.10	1.25
k_{17}/kg·mol^{-1}·min^{-1}	90.43	96.23	k_{36}/kg·mol^{-1}·min^{-1}	3.37	0.30
k_{18}/kg·mol^{-1}·min^{-1}	90.45	90.96	k_{37}/min^{-1}	29.98	29.12
k_{19}/kg·mol^{-1}·min^{-1}	90.46	90.94			

During the chain initiation stage, the chain initiation rate (k_1) of the STRATCO technology is higher than that of the SINOALKY technology. STRATCO employs a high-shear impeller and an internal circulation design (with a circulation flow rate of 425 t/h) to enhance the acid–hydrocarbon mixing efficiency, thereby accelerating the protonation of butene to generate carbocation. In contrast, SINOALKY relies on static mixers, which results in a lower local mixing intensity and consequently a slightly lower chain initiation rate. The reverse chain initiation rate (k_2) of STRATCO is lower than that of SINOALKY. The SINOALKY technology employs an adiabatic reactor, where the reaction temperature increases along the reactor length due to the exothermic nature of the alkylation reaction. Elevated temperatures thermodynamically disfavor the forward reaction by shifting the chemical equilibrium away from the desired products. Additionally, the multi-stage dilution design prolongs the survival time of the carbocation in the acid phase, allowing partial deprotonation of the carbocation back to butene, thereby resulting in a slightly

higher reverse reaction rate. The stirred impeller in STRATCO requires higher energy consumption compared to the static mixer in SINOALKY. However, the reaction effluent in the tube side of STRATCO effectively removes heat from the reaction mixture in the shell side. These features collectively render STRATCO more favorable for facilitating the chain initiation process than SINOALKY.

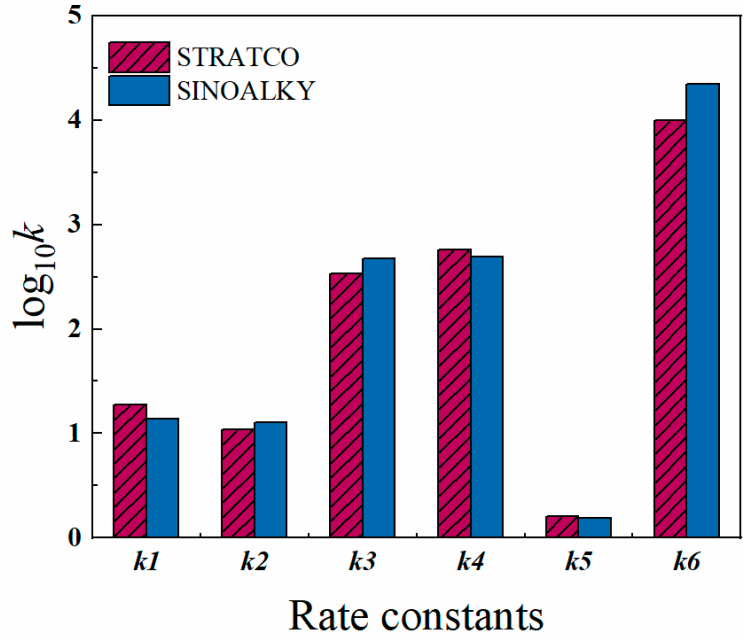


Figure 6. Comparison between the key rate constants for STRATCO and SINOALKY technologies.

During the chain propagation stage, the reaction rate constant (k_4) for the addition of tert-butyl carbocation to isobutene to form TMP^+ in the STRATCO technology is higher than that in the SINOALKY technology. This is attributed to STRATCO's high circulation flow rate, which shortens the diffusion time of the carbocations in the acid phase, thereby promoting their rapid engagement in chain propagation reactions. In contrast, SINOALKY's multi-stage reactor design extends the axial residence time, allowing some carbocations to undergo side reactions such as isomerization or cracking, which reduces the selectivity toward the desired chain propagation pathways. In the SINOALKY technology, the reaction rates (k_3 and k_6) for forming TMP^+ and DMH^+ with the addition of tert-butyl carbocations to 2-butene and 1-butene, respectively, are higher than those in the STRATCO technology. This enhancement arises from SINOALKY's multi-stage feeding strategy, which dilutes the local concentration of butene, thereby directing the olefin to preferentially engage in chain propagation with carbocations.

During the chain termination stage, the rate constant for TMP formation (k_5) in the STRATCO technology is higher than that in the SINOALKY technology, while the rate constant for DMH formation (k_7) is slightly lower. TMP, an ideal high-octane product, is generated through the hydrogen transfer reaction between carbocation and isobutane. A higher k_5 value directly correlates with enhanced TMP selectivity and a superior RON of the alkylate. In contrast, DMH, a lower-octane C_8 isomer, predominantly forms isomerization or alternative chain propagation pathways of carbocation. An elevated k_7 value increases the DMH fraction, thereby reducing the overall octane number of the product. STRATCO achieves a high k_5 value by maintaining elevated isobutane concentrations through internal circulation (425 t/h), thereby promoting the hydride transfer reaction between the carbocation and isobutane for selective TMP formation. Conversely, SINOALKY's strategy of supplemental feeding in the second stage dilutes the butene concentration to suppress side

reactions but slightly reduces the local isobutane concentration in the acid phase, thereby moderating the chain termination efficiency for TMP formation.

The rate constants for the four side reactions (k_{24}, k_{25}, k_{28}, and k_{29}) in the SINOALKY technology are significantly higher than those in the STRATCO technology, indicating a greater propensity for generating higher-carbon byproducts such as C_9 and C_{11}. This discrepancy arises from SINOALKY's strategy of supplemental feeding in the second stage, which dilutes the butene concentration but may lead to localized accumulation of intermediates (e.g., C_5^+ and C_7^+) in specific regions, such as near the outlet of static mixers, due to uneven mass transfer. The localized enrichment of intermediates promotes undesired addition reactions.

In both the STRATCO and SINOALKY technologies, the parameters in the chain propagation stage (k_3, k_4, k_6) are significantly higher than those in the chain initiation (k_1) and chain termination (k_5, k_7) stages. The high circulation flow rate in STRATCO and the static mixer design in SINOALKY both shorten the diffusion time of the carbocations in the acid phase, ensuring their rapid participation in chain propagation.

The two technologies adopt the same catalyst (sulfuric acid), as well as similar raw materials (isobutane and butene) and operating conditions (such as the temperature, pressure, and acid concentration), so their kinetic parameters exhibit a certain degree of similarity.

Although there are differences in reactor design (such as the internal circulation flow design in STRATCO and the vertical multi-stage design in SINOALKY) that can affect the local mass transfer efficiency, the reaction behavior of the alkylation system is still dominated by the same carbocation pathway.

The sensitivity analysis of rate constants on the C_8 mass fraction for the STRATCO and SINOALKY reactors was performed, as shown in Table 5. The operational parameters for both technologies are configured as follows.

Table 5. A sensitivity analysis of rate constants on C_8 mass fractions for the STRATCO and SINOALKY reactors.

Sensitivity Coefficients	STRATCO	SINOALKY	Sensitivity Coefficients	STRATCO	SINOALKY
S_1	6.36×10^{-2}	7.27×10^{-3}	S_{20}	-1.37×10^{-2}	-8.54×10^{-4}
S_2	-5.56×10^{-2}	-6.93×10^{-3}	S_{21}	-6.07×10^{-2}	-5.63×10^{-3}
S_3	1.01×10^{-2}	4.55×10^{-4}	S_{22}	-2.93×10^{-4}	-6.31×10^{-5}
S_4	6.70×10^{-2}	2.51×10^{-3}	S_{23}	-2.22×10^{-3}	-4.33×10^{-4}
S_5	7.11×10^{-2}	8.72×10^{-3}	S_{24}	-4.23×10^{-4}	-8.66×10^{-5}
S_6	-9.62×10^{-2}	1.53×10^{-3}	S_{25}	-6.35×10^{-3}	-4.13×10^{-4}
S_7	3.20×10^{-2}	9.68×10^{-4}	S_{26}	-3.24×10^{-4}	-4.63×10^{-5}
S_8	-9.23×10^{-3}	-2.66×10^{-4}	S_{27}	-1.68×10^{-3}	-2.69×10^{-4}
S_9	-9.11×10^{-4}	-3.59×10^{-5}	S_{28}	-2.09×10^{-4}	-3.04×10^{-5}
S_{10}	-1.86×10^{-4}	-7.63×10^{-5}	S_{29}	-3.36×10^{-3}	-1.26×10^{-4}
S_{11}	-2.78×10^{-5}	-1.17×10^{-5}	S_{30}	-9.86×10^{-5}	-1.72×10^{-5}
S_{12}	-3.35×10^{-2}	-6.10×10^{-3}	S_{31}	1.30×10^{-3}	1.40×10^{-4}
S_{13}	-5.11×10^{-3}	-9.23×10^{-4}	S_{32}	-6.37×10^{-5}	-5.36×10^{-6}
S_{14}	-2.67×10^{-3}	-4.76×10^{-4}	S_{33}	-1.86×10^{-2}	-3.22×10^{-4}
S_{15}	-3.74×10^{-4}	-6.91×10^{-5}	S_{34}	3.84×10^{-3}	4.42×10^{-4}
S_{16}	-9.12×10^{-3}	-6.23×10^{-4}	S_{35}	7.50×10^{-4}	1.52×10^{-4}
S_{17}	-3.98×10^{-2}	-4.18×10^{-3}	S_{36}	1.86×10^{-3}	2.09×10^{-4}
S_{18}	-2.60×10^{-4}	-4.73×10^{-5}	S_{37}	-1.93×10^{-3}	-2.10×10^{-4}
S_{19}	-1.73×10^{-3}	-3.25×10^{-4}			

For the STRATCO technology, three parallel reactors (A, B, and C) are utilized. Each reactor operates under the following conditions: a fresh feed flow rate of 30 t/h, inlet temperature of 3.5 °C, isobutane-to-olefin molar ratio of 10:1, internal circulation flow rate of 425 t/h, and acid-to-hydrocarbon volume ratio of 1.1:1. Reactors A and B maintain

an acid concentration of 94 wt%, while reactor C employs acid from the preceding reactors, resulting in a reduced concentration of 92 wt%. In the SINOALKY technology, a two-stage reactor configuration is adopted. The total fresh feed flow rate is 100 t/h, with a 2:1 ratio allocated between the first and second stages. The first stage of the reactor operates at an inlet temperature of 3.5 °C, isobutane-to-olefin molar ratio of 10:1, recycled hydrocarbon flow rate of 506 t/h, acid-to-hydrocarbon volume ratio of 1.1:1, and acid concentration of 92 wt%. The sensitivity coefficients are defined as $S = \ln(m_2/m_1)/\ln(k_{mod}/k_{orig})$, where k_{orig} is the rate constant of the original reaction; k_{mod} is the rate constant, which is twice the value of k_{orig}; and m_2 and m_1 are the C_8 mass fractions corresponding to the reaction rate constants k_{mod} and k_{orig}, respectively [38]. For this sensitivity coefficients definition, a positive sensitivity coefficient stands for the effect on promoting C_8 formation, whereas a negative sensitivity coefficient stands for the inhibition effect.

The sensitivity coefficient analysis in Table 5 reveals that in both STRATCO and SINOALKY technologies, the chain initiation reaction (k_1), reverse chain initiation reaction (k_2), and chain termination reaction between C_8 carbocations and isobutane (k_5) significantly influence C_8 formation. In the STRATCO technology, the high sensitivity coefficients of k_1 and k_5 originate from its high-shear impeller and internal circulation design, which enhance the protonation efficiency of butene and stabilize the hydride transfer reaction, thereby accelerating carbocation generation. In contrast, the SINOALKY technology employs a multi-stage feeding strategy that dilutes the butene concentration to mitigate carbocation accumulation risks. These findings indicate that optimizing the C_8 selectivity requires enhancing k_1 and k_5 to be enhanced while suppressing k_2.

4.2. Model Validation

To verify the reliability of the established kinetic model and the determined model parameters, the left 10 sets and 5 sets of industrial data that were not involved in parameter estimation were selected for the STRATCO and SINOALKY reactors, respectively. The reliability of the two reactor models was judged by the deviation between the model-predicted calculated values and the actual values. For the STRATCO reactor, the average relative deviations of C_5, C_6, C_7, C_8, C_9, C_{10}, and C_{11} are 7.06%, 4.79%, 4.81%, 1.72%, 15.89%, 17.43%, and 10.22%, respectively; for the SINOALKY reactor, the average relative deviations are 5.21%, 2.68%, 3.30%, 1.73%, 1.93%, 4.26%, and 4.07%, respectively. The average temperature difference between the predicted calculated value and the actual value of the SINOALKY reactor outlet temperature is 0.15 °C. The deviations between the calculated and experimentally determined alkylate oil component mass fractions for both technologies are presented in Figures 7 and 8. The verification results indicate that the kinetic model and kinetic parameters are reliable, enabling accurate prediction of the product distribution of industrial alkylation units.

4.3. Model Prediction

4.3.1. Concentration Profile of the Reactor

Based on the established model, the axial evolution of alkylation products along the reactor length can be predicted. The operational parameters for both processes are configured as follows.

For the STRATCO process, three parallel reactors (A, B, and C) are utilized. Each reactor operates under the following conditions: a fresh feed flow rate of 40 t/h, inlet temperature of 3.5 °C, isobutane-to-olefin molar ratio of 10:1, internal circulation flow rate of 425 t/h, and acid-to-hydrocarbon volume ratio of 1.1:1. Reactors A and B maintain an acid concentration of 94 wt%, while reactor C employs acid from the preceding reactors, resulting in a reduced concentration of 92 wt%. In the SINOALKY process, a two-stage

reactor configuration is adopted. The total fresh feed flow rate is 120 t/h, with a 2:1 ratio allocated between the first and second stages. The first stage of the reactor operates at an inlet temperature of 3.5 °C, isobutane-to-olefin molar ratio of 10:1, recycled hydrocarbon flow rate of 506 t/h, acid-to-hydrocarbon volume ratio of 1.1:1, and acid concentration of 92 wt%.

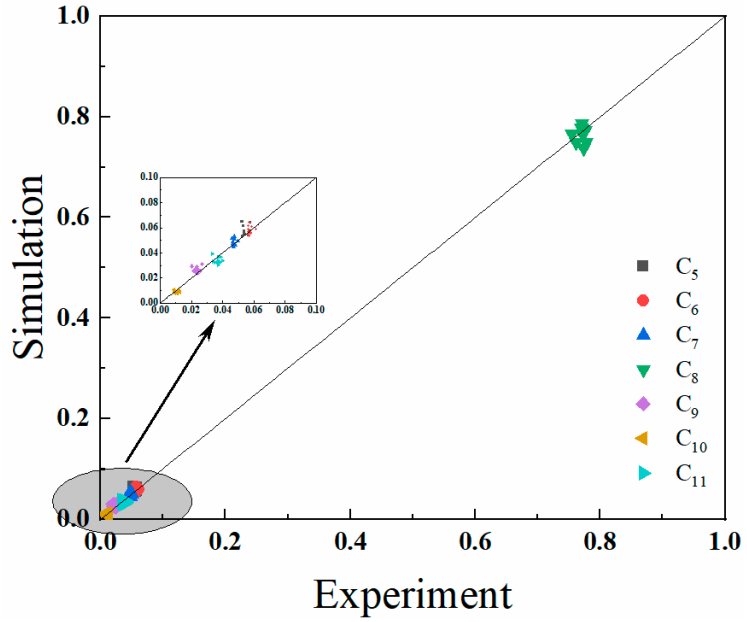


Figure 7. Deviation distribution of component mass fractions of STRATCO alkylated oil.

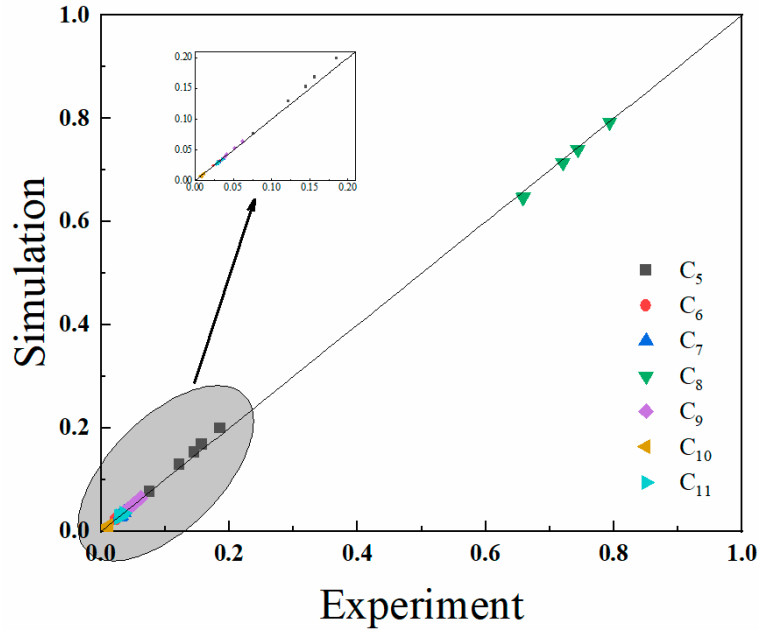


Figure 8. Deviation distribution of component mass fractions of SINOALKY alkylated oil.

The concentration profiles of C_8 and the intermediate products along the reactor length are illustrated in Figure 9. The results indicate that in both reactor systems, the C_8 concentration increases rapidly with the reactor length (residence time) before stabilizing, while intermediate products initially accumulate and subsequently decline. This behavior reflects the dominance of chain initiation and propagation in the early stages, leading to intermediate accumulation, followed by gradual consumption when chain termination reactions dominate with prolonged residence times, thereby slowing the C_8 formation.

Both reactors exhibit similar trends due to having the same carbocation mechanism. In the STRATCO configuration, reactor C operates with a slightly lower acid concentration (1–2 wt% less than reactors A and B). When the sulfuric acid concentration decreases, the catalytic activity of the acid phase weakens, which adversely affects the generation and stability of the carbocations. This delays the combination of carbocations with isobutane to form the target product C_8 and leads to the accumulation of unconsumed carbocation intermediates. These intermediates subsequently participate in side reactions such as isomerization or cracking, resulting in reduced C_8 selectivity in the reactor. Additionally, under low sulfuric acid concentrations, the protonation efficiency of the olefins declines, leaving the butene molecules more prone to oligomerization reactions. This consumes olefins that would otherwise contribute to alkylation. In the SINOALKY process, the concentration of the main product C_8 at the inlet of the second stage of the reactor decreases compared to the outlet of the first stage, with a reduced magnitude of change. The alkylation products from the first stage of the reactor are blended with fresh C_8-free feedstock prior to entering the second reactor stage, resulting in a reduced concentration of C_8 at the second reactor inlet. Furthermore, as the fresh feedstock flow rate in the second stage is maintained at half the inlet flow rate of the first reactor, the diluted olefin concentration in the mixed feed stream leads to a suppressed rate of the primary alkylation reaction. Concurrently, the carbocation intermediates generated during the alkylation process undergo competing side reactions, including addition and cracking pathways.

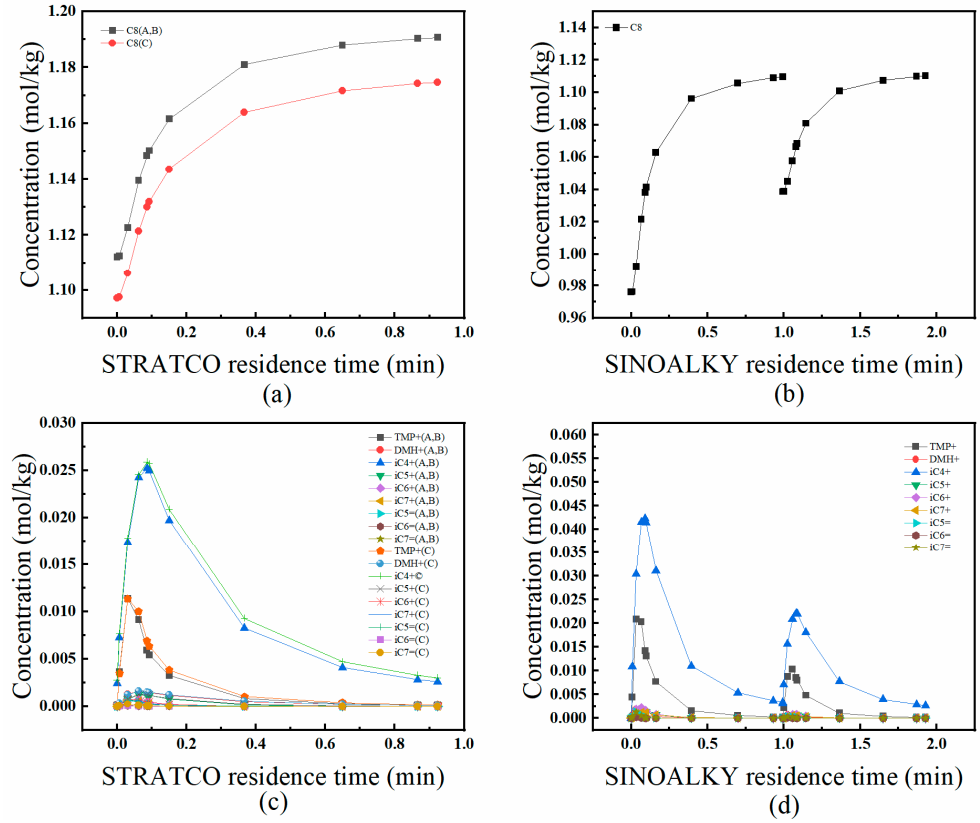


Figure 9. Analysis of the changes of C_8 (**a**,**b**) and carbocation (**c**,**d**) components along the reactor tube length.

4.3.2. Effect of Space–Time

Space–time, a critical parameter reflecting the industrial production capacity, directly influences the selectivity of the main product C_8. This parameter can be modulated by adjusting the flow rate of the fresh feed. To evaluate the impact of space–time on the C_8

selectivity and octane number of the final alkylate oil, the operational conditions for both processes were configured as follows. For the STRATCO process, each reactor operated with fresh feed flow rates ranging from 60 to 70 t/h, and the outlet product streams from the three reactors were combined into a single product stream. In the SINOALKY process, the total fresh feed flow rate was maintained between 100 and 120 t/h, with other operating parameters consistent with those specified in Section 4.3.1

Both processes achieved butene conversion rates exceeding 99%, with the C_8 selectivity and octane number of the alkylate shown in Figure 10. The results demonstrate that as the space–time decreases, both the C_8 selectivity and alkylate octane number decline in the two reactor systems. Variations in the fresh feed flow rate have a relatively minor impact on the actual space–time. In the STRATCO process, the internal circulation flow rate (425 t/h) is significantly higher than the fresh feed flow rate (30–70 t/h). Similarly, in the SINOALKY process, the external hydrocarbon circulation (500–650 t/h) results in a low proportion of fresh feed flow (110–130 t/h) relative to the total flow. An increase in the fresh feed flow rate reduces the isobutane-to-olefin ratio and elevates the unit load. The lowered isobutane-to-olefin ratio increases the probability of butene participating in oligomerization side reactions, thereby adversely affecting the progression of the main reaction.

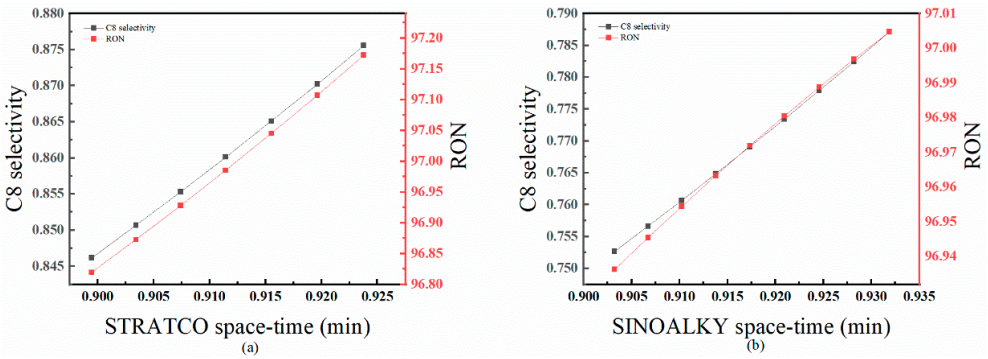


Figure 10. Effect of space–time on C_8 selectivity and alkylate octane number in STRATCO (**a**) and SINOALKY (**b**) reactors.

4.3.3. Effect of Isobutane-to-Olefin Ratio

In alkylation processes, the isobutane-to-olefin molar ratio serves as a critical parameter for regulating product distribution. The STRATCO and SINOALKY processes were operated with fresh feed flow rates of 30, 50, and 70 t/h and 100, 120, and 140 t/h, respectively. To investigate the influence of the isobutane-to-olefin ratio on the C_8 selectivity and alkylate octane number, both processes were operated with isobutane-to-olefin ratios ranging from 9:1 to 10:2, while maintaining other conditions consistent with those detailed in Section 4.3.1.

Both processes achieved butene conversion rates exceeding 99%, with the C_8 selectivity and octane number of the alkylate shown in Figure 11. The results indicate that moderately increasing the isobutane-to-olefin molar ratio optimizes the alkylation performance in both reactor systems, enhancing the C_8 selectivity and octane number. A higher isobutane-to-olefin ratio effectively suppresses side reactions by diluting the local olefin concentration. When increasing this ratio, the SINOALKY process exhibited smaller variations in C_8 selectivity compared to the STRATCO process. This reduced sensitivity stems from SINOALKY's multi-stage feeding design, which maintains lower butene concentrations in the hydrocarbon phase at the second stage inlet.

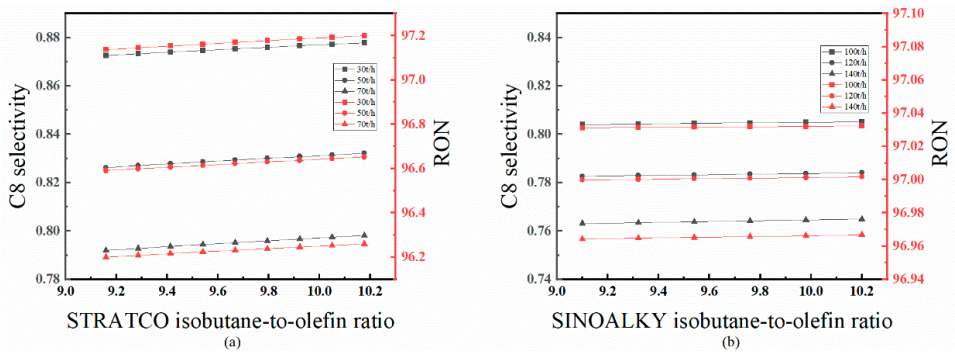


Figure 11. Effect of isobutane-to-olefin ratio on C_8 selectivity and alkylate octane number in STRATCO (**a**) and SINOALKY (**b**) reactors.

4.3.4. Effect of Acid-to-Hydrocarbon Ratio

The acid-to-hydrocarbon ratio regulates the product selectivity and alkylate octane number by modulating the relative proportions of acid and hydrocarbons in the reaction system. The STRATCO and SINOALKY processes were operated with fresh feed flow rates of 30, 50, and 70 t/h and 100, 120, and 140 t/h, respectively. To evaluate the impact of this ratio on the C_8 selectivity and octane performance, both processes were operated with acid-to-hydrocarbon ratios ranging from 0.8 to 1.4, while maintaining all other conditions consistent with those described in Section 4.3.1.

The butene conversion rates of both processes exceed 99%, while the C_8 selectivity and octane number of the alkylate are presented in Figure 12. The results demonstrate that an appropriate increase in acid-to-hydrocarbon ratio could enhance both the C_8 selectivity and octane number for both reactor systems. This observation aligns with the correction function integrated into the kinetic model, where a higher acid-to-hydrocarbon ratio improves the selectivity of primary alkylation pathways, thereby optimizing the C_8 product distribution. When increasing the acid-to-hydrocarbon ratio, STRATCO exhibits smaller variations in C_8 selectivity compared to SINOALKY. This reduced sensitivity is attributed to STRATCO's internal circulation, which enhances the acid–hydrocarbon mixing efficiency and maintains sufficient interfacial contact under varying acid-to-hydrocarbon ratios. The design mitigates the impact of acid-to-hydrocarbon ratio fluctuations on C_8 selectivity.

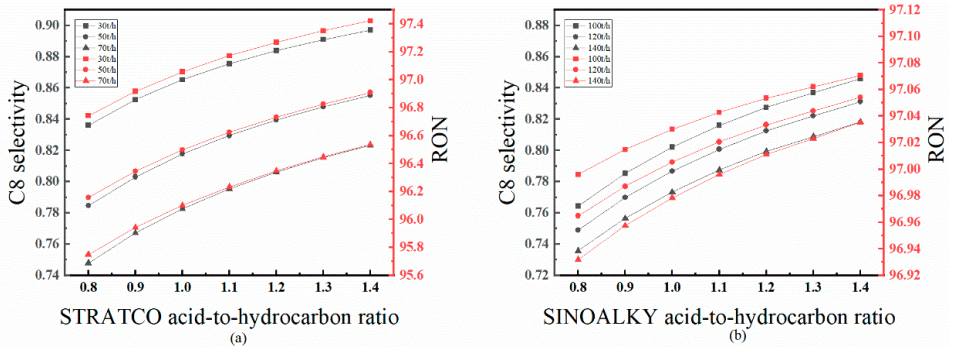


Figure 12. Effect of acid-to-hydrocarbon ratio on C_8 selectivity and alkylate octane number in STRATCO (**a**) and SINOALKY (**b**) reactors.

5. Conclusions

(1) Based on the carbocation reaction mechanism, a kinetic model for sulfuric acid-catalyzed isobutane–butene alkylation was established, including 20 lumped components and 37 reaction pathways. Reactor models tailored to the design features of STRATCO and SINOALKY alkylation technologies were subsequently developed. The validation against the industrial data confirmed the model's accuracy. The model validation demonstrated

average relative deviations of 1.72% and 1.73% for C_8 product predictions for the STRATCO and SINOALKY technologies, respectively, showing excellent agreement with the industrial values. Through a parameter analysis, the crucial role of the reactor design (such as the circulation flow rate of the STRATCO technology and multi-stage feeding of the SINOALKY technology) in the primary alkylation reaction was revealed.

(2) The model was applied to assess the effects of the operating conditions on the alkylate quality. The simulation results showed that increasing the space–time, isobutane-to-olefin ratio, and acid-to-hydrocarbon ratio enhanced the alkylation performance. It was also found that the internal circulation in the STRATCO technology enables thorough contact between the acid and hydrocarbon phases, while the multi-stage feeding in the SINOALKY technology maintains a favorable isobutane-to-olefin ratio. Both features are conducive to the alkylation reaction. These findings align with the intrinsic reaction mechanisms of sulfuric acid alkylation systems. The quantitative relationships derived from this study provide critical guidance for optimizing the operating conditions in STRATCO and SINOALKY industrial units, ensuring robust process control under variable conditions and reinforcing sulfuric acid alkylation as a sustainable pillar in low-sulfur fuel product.

The modelling methodology proposed in this work (e.g., lumped kinetic network construction, equation-oriented method) remains feasible for other alkylation technologies (e.g., solid–acid or ionic-liquid-catalyzed alkylation), although reengineering the framework to account for distinct reactor configurations is necessary.

Author Contributions: Conceptualization, H.J.; methodology, H.J.; validation, W.Z.; formal analysis, W.Z.; writing—original draft preparation, W.Z.; writing—review and editing, H.J., W.Z.; project administration, H.J. All authors have read and agreed to the published version of the manuscript.

Funding: This research received no external funding.

Data Availability Statement: The original contributions presented in this study are included in the article. Further inquiries can be directed to the corresponding author.

Conflicts of Interest: The authors declare no conflict of interest.

Abbreviations

The following abbreviations are used in this manuscript:

RON	Research octane number
TMP	Trimethylpentane
DMH	Dimethylhexane
SM	Sequential modular method
EO	Equation-oriented method

References

1. Zhu, Q.Y.; Zheng, L.J.; Ren, W.P. New progress in alkylate oil production technologies. *Petrochem. Technol. Appl.* **2016**, *34*, 511–515.
2. Zhu, Q.Y.; Qiao, M.; Ren, J. Trend in Technology of Gasoline Alkylated with Liquid Acid. *Petrochem. Ind. Technol.* **2010**, *17*, 49–53.
3. Sun, H.; Song, Y.; Zhou, X.; He, M.; Ali, M.F.; Rizwan, M. Study on Isobutane/1-Butene Alkylation over Phosphorus-Modified HY Zeolite. *Catal. Lett.* **2024**, *154*, 651–663. [CrossRef]
4. Zhang, H.K. Current status and progress of C_4 alkylation technology. *Qilu Petrochem. Technol.* **2022**, *50*, 242–248.
5. Li, Q.; Chi, Z.M.; Zhu, D.L. Research progress in the alkylation technology. *Contemp. Chem. Ind.* **2016**, *45*, 2440–2442.
6. Li, W. Study on the C_4 Alkylation Reaction Catalyzed by Ionic Liquid/Solid Acid Catalysts. Master's Thesis, Inner Mongolia University, Hohhot, China, 2018.
7. Ma, L.L.; Xu, H.G.; Gao, C. Summary for industry application of alkylation technology. *Technol. Dev. Chem. Ind.* **2013**, *42*, 24–27.
8. Dang, X.F.; Shi, F.Y.; Wang, Y.B. The comparison of sulfuric acid and hydrofluoric acid alkylation technology. *Pet. Plan. Eng.* **2018**, *29*, 14–17.

9. Ma, Z.; Zheng, W.; Dong, M.; Sun, W.; Zhao, L. Assessing industrial-scale H_2SO_4-catalyzed C_4 alkylation enhanced by $[N_{1,1,1,1}][C_{10}SO_4]$ additives based on a complex kinetic model. *Ind. Eng. Chem. Res.* **2024**, *63*, 2177–2186. [CrossRef]
10. Albright, L.F.; Li, K.W. Alkylation of isobutane with light olefins using sulfuric acid reaction mechanism and comparison with HF alkylation. *Ind. Eng. Chem. Process Des. Dev.* **1970**, *9*, 447–454. [CrossRef]
11. Albright, L.F.; Doshi, B.M.; Ferman, M.A.; Ewo, A. *Alkylation of Isobutane with C_4 Olefins*; American Chemical Society: Washington, DC, USA, 1977.
12. Mi, H.G. Analysis of factors of sulfuric acid alkylation reaction. *Chem. Enterp. Manag.* **2020**, *13*, 94–95.
13. Fu, K.; Chen, X.; Chen, Z.; Wu, C.; Wei, X.; Liang, J.; Nong, W.; Wang, L. Response surface methodology optimization and kinetic study of isobutene/2-butene alkylation reaction. *React. Kinet. Mech. Catal.* **2023**, *136*, 1891–1913. [CrossRef]
14. Ivashkina, E.; Dolganova, I.; Dolganov, I.; Ivanchina, E.; Nurmakanova, A.; Bekker, A. Modeling the H_2SO_4-catalyzed isobutane alkylation with alkenes considering the process unsteadiness. *Catal. Today* **2019**, *329*, 206–213. [CrossRef]
15. Geng, Y.J. *Alkylation Process and Technology*; China Petrochemical Press: Beijing, China, 1993.
16. Schmerling, L. The mechanism of the alkylation of paraffins. *J. Am. Chem. Soc.* **1945**, *67*, 1778–1783. [CrossRef]
17. Langley, J.R.; Pike, R.W. The kinetics of alkylation of isobutane with propylene. *AIChE J.* **1972**, *18*, 698–705. [CrossRef]
18. Lee, L.M.; Harriott, P. The kinetics of isobutane alkylation in sulfuric acid. *Ind. Eng. Chem. Process Des. Dev.* **1977**, *16*, 282–287. [CrossRef]
19. Sun, W.; Shi, Y.; Chen, J.; Xi, Z.; Zhao, L. Alkylation kinetics of isobutane by C_4 olefins using sulfuric acid as catalyst. *Ind. Eng. Chem. Res.* **2013**, *52*, 15262–15269. [CrossRef]
20. Xin, Z.C.; Jiang, H.B.; Zhang, Z.; Chen, Y.; Wang, J. Kinetic model of olefins/isobutane alkylation using sulfuric acid as catalyst. *ACS Omega* **2022**, *7*, 9513–9526. [CrossRef] [PubMed]
21. Kranz, K. Cold Temperature Alkylation Process. U.S. Patent 5,095,168, 8 November 1989.
22. Meyers, R.A. *Handbook of Petroleum Refining Processes*; McGrawHill: New York, NY, USA, 2003.
23. Zhang, Q.X. Introduction of STRATCO sulfuric acid alkylation reactor. *Petrochem. Equip. Technol.* **1991**, *1*, 21.
24. Dong, M.H.; Zong, B.N. Sinoalky technology for sulfuric acid alkylation and its application. *Pet. Process. Petrochem.* **2019**, *50*, 29–32.
25. Cai, H.B.; Dai, G.C. CFD Simulation of Fluid Flow in Sulfuric Acid Alkylation Reactor—Effect of Structure Parameters. *Chem. React. Eng. Technol.* **2012**, *28*, 391–397.
26. Zhang, L.; Xu, Z.M.; Yuan, X.Q. *Principles of Chemical Reaction Engineering*; East China University of Science and Technology Press: Shanghai, China, 2007.
27. Nurmakanova, A.E.; Ivashkina, E.N.; Ivanchina, E.; Dolganov, I.; Boychenko, S. Predicting alkylate yield and its hydrocarbon composition for sulfuric acid catalyzed isobutane alkylation with olefins using the method of mathematical modeling. *Procedia Chem.* **2015**, *15*, 54–64. [CrossRef]
28. Ma, P.S. *Data Manual for Experimental Physical Properties of Organic Compounds*; Chemical Industry Press: Beijing, China, 2006.
29. Editorial Committee of the Sulfuric Acid Association. *Sulfuric Acid Manual*; Chemical Industry Press: Beijing, China, 1982.
30. Cao, P.; Zheng, L.; Sun, W.Z.; Zhao, L. Multiscale Modeling of Isobutane Alkylation with Mixed C_4 Olefins Using Sulfuric Acid as Catalyst. *Ind. Eng. Chem. Res.* **2019**, *58*, 6340–6349. [CrossRef]
31. Wang, P.; Wang, D.; Xu, C.; Gao, J. DFT calculations of the alkylation reaction mechanisms of isobutane and 2-butene catalyzed by Bronsted acid. *Appl. Catal. A Gen.* **2007**, *332*, 22–26. [CrossRef]
32. Rodríguez, M.A.; Ancheyta, J. Detailed description of kinetic and reactor modeling for naphtha catalytic reforming. *Fuel* **2011**, *90*, 3492–3508. [CrossRef]
33. Lanczos, C. Trigonometric Interpolation of Empirical, Analytical Functions. *Stud. Appl. Math.* **1938**, *17*, 85–88. [CrossRef]
34. Villadsen, J.V.; Stewart, W.E. Solution of Boundary-value Problems by Orthogonal Collocation. *Chem. Eng. Sci.* **1995**, *22*, 1483–1501. [CrossRef]
35. Jiang, H.B.; Sun, Y.; Jiang, S.B.; Li, Z.M.; Tian, J.H. Reactor model of counter-current continuous catalyst-regenerative reforming process toward real time optimization. *Energy Fuels* **2021**, *35*, 10770–10785. [CrossRef]
36. Li, D.; Sun, W.; Xi, Z.; Zhang, M.; Zhao, L. Alkylation kinetics of mixed butenes/isobutane by sulfuric acid. *CIESC J.* **2015**, *66*, 584–590.
37. Ma, Q.F. Analysis and optimization of influencing factors on product quality of sulfuric acid alkylation. *Chem. Enterp. Manag.* **2019**, *15*, 38–39.
38. Yu, J.; Gou, X.L.; Yu, J.J. Comprehensive Chemical Kinetic Model of 2,6,10-Trimethyl Dodecane. *Energy Fuels* **2020**, *34*, 2366–2375. [CrossRef]

Disclaimer/Publisher's Note: The statements, opinions and data contained in all publications are solely those of the individual author(s) and contributor(s) and not of MDPI and/or the editor(s). MDPI and/or the editor(s) disclaim responsibility for any injury to people or property resulting from any ideas, methods, instructions or products referred to in the content.